Published in final edited form as:

Clin Cancer Res. 2020 November 15; 26(22): 6017–6027. doi:10.1158/1078-0432.CCR-20-1916.

Concentration-dependent early anti-vascular and anti-tumor effects of itraconazole in non-small cell lung cancer

David E. Gerber[1,2,3], **William T. Putnam**[4], **Farjana J. Fattah**[1], **Kemp H. Kernstine**[1,5], **Rolf A. Brekken**[1,6,7], **Ivan Pedrosa**[8], **Rachael Skelton**[1], **Jessica M. Saltarski**[1], **Robert E. Lenkinski**[8], **Richard Leff**[4], **Chul Ahn**[1,3], **Chyndhri Padmanabhan**[1], **Vaidehi Chembukar**[1], **Sahba Kasiri**[7], **Raja Reddy Kallem**[4], **Indhumathy Subramaniyan**[4], **Qing Yuan**[8], **Quyen N. Do**[8], **Yin Xi**[8], **Scott I. Reznik**[5], **Lorraine Pelosof**[1,*], **Brandon Faubert**[9], **Ralph J. DeBerardinis**[9,10], **James Kim**[1,2,7]

[1]Harold C. Simmons Comprehensive Cancer Center, University of Texas Southwestern Medical Center, Dallas, TX, USA;

[2]Department of Internal Medicine (Division of Hematology-Oncology), University of Texas Southwestern Medical Center, Dallas, TX, USA;

[3]Department of Population and Data Sciences, University of Texas Southwestern Medical Center, Dallas, TX, USA;

[4]Department of Pharmacy Practice, Jerry H. Hodge School of Pharmacy, Texas Tech University Health Sciences Center, Dallas, TX, USA;

[5]Department of Cardiovascular and Thoracic Surgery., University of Texas Southwestern Medical Center, Dallas, TX, USA;

[6]Department of Surgery, University of Texas Southwestern Medical Center, Dallas, TX, USA;

[7]Hamon Center for Therapeutic Oncology Research, University of Texas Southwestern Medical Center, Dallas, TX, USA;

[8]Department of Radiology, University of Texas Southwestern Medical Center, Dallas, TX, USA

[9]Children's Research Institute, University of Texas Southwestern Medical Center, Dallas, TX, USA

Full Address for Correspondence: David E. Gerber, MD, Division of Hematology-Oncology, Harold C. Simmons Comprehensive Cancer Center, University of Texas Southwestern Medical Center, 5323 Harry Hines Blvd., Mail Code 8852, Dallas, TX 75390-8852, USA, Telephone: +1 214-648-4180, Fax: +1 214-648-1955, david.gerber@utsouthwestern.edu.

*Dr. Pelosof is now at the U.S. Food and Drug Administration (FDA). Dr. Pelosof contributed to this research while employed at UTSW. Her current affiliation is the FDA. The views expressed in this paper should not be construed to reflect the views or policies of the FDA.

Disclosures:

The authors have no relevant disclosures.

Statement of Translational Relevance:

Angiogenesis targeting has emerged as therapeutically relevant to lung cancer, including in the setting of immune checkpoint inhibition and epidermal growth factor receptor (EGFR) inhibition. Preclinical work from our group and others has shown that the anti-fungal agent itraconazole inhibits angiogenesis, the Hedgehog (Hh) pathway, and tumor growth. In the present study, we performed a pre-operative, window-of-opportunity trial of fixed-dose itraconazole in early-stage non-small cell lung cancer (NSCLC). We found that both plasma and intra-tumoral itraconazole concentrations varied widely among patients. Furthermore, itraconazole levels were significantly and meaningfully correlated with changes in tumor volume, tumor perfusion, angiogenic cytokines, and tumor microvessel density. Itraconazole-treated tumors also demonstrated distinct metabolic profiles, but itraconazole did not appear to inhibit the Hh pathway. This study demonstrates concentration-dependent early anti-vascular and anti-tumor effects of itraconazole. As the number of fixed-dose cancer therapies increases, attention to inter-patient pharmacokinetic and pharmacodynamic differences may be warranted.

[10]Howard Hughes Medical Institute, University of Texas Southwestern Medical Center, Dallas, TX, USA

Abstract

Introduction: Itraconazole has been repurposed as an anti-cancer therapeutic agent for multiple malignancies. In preclinical models, itraconazole has antiangiogenic properties and inhibits Hedgehog (Hh) pathway activity. We performed a window-of-opportunity trial to determine the biologic effects of itraconazole in human patients.

Methods: Patients who had non-small cell lung cancer planned for surgical resection were administered 10–14 days of itraconazole 300 mg orally twice daily. Patients underwent dynamic contrast-enhanced MRI and plasma collection for pharmacokinetic (PK) and pharmacodynamic analyses. Tissue from pre-treatment biopsy, surgical resection, and skin biopsies were analyzed for itraconazole and hydroxyitraconazole concentration, and vascular and Hh pathway biomarkers.

Results: Thirteen patients were enrolled. Itraconazole was well tolerated. Steady state plasma concentrations of itraconazole and hydroxyitraconazole demonstrated a six-fold difference across patients. Tumor itraconazole concentrations trended with and exceeded those of plasma. Greater itraconazole levels were significantly and meaningfully associated with reduction in tumor volume (Spearman correlation −0.71; P=0.05) and tumor perfusion (K^{trans}) (correlation −0.71; P=0.01), decreases in the pro-angiogenic cytokines interleukin 1b (correlation −0.73; P=0.01) and GM-CSF (correlation −1.00; P<0.001), and reduction in tumor microvessel density (correlation −0.69; P=0.03). Itraconazole-treated tumors also demonstrated distinct metabolic profiles. Itraconazole treatment did not alter transcription of *GLI1* and *PTCH1* mRNA. Patient size, renal function, and hepatic function did not predict itraconazole concentrations.

Conclusions: Itraconazole demonstrates concentration-dependent early anti-vascular, metabolic, and anti-tumor effects in patients with NSCLC. As the number of fixed-dose cancer therapies increases, attention to inter-patient PK and pharmacodynamic differences may be warranted.

NCT02357836

Keywords

Angiogenesis; Hedgehog; Pharmacokinetics; Metabolomics; Neoadjuvant; Repurpose; Vascular

---

Repurposing of clinically available pharmaceuticals provides an efficient and cost-effective means of bringing new treatments to patients. By bypassing animal toxicology and human dose-finding studies, this approach allows researchers and clinicians to advance their findings directly from proof-of-principle *in vitro* and *in vivo* studies to efficacy evaluations in patients. Successful examples of repurposed pharmaceutical agents include aspirin (employed as an analgesic for decades before its use to prevent and treat cardiovascular disease) and hydroxychloroquine (an antimalarial found to have immune modulating properties for the treatment of systemic lupus erythematosis and other autoimmune conditions) (1).

In oncology, several medical therapies in use for other conditions have been explored and in some cases established as anti-cancer agents. Among others, examples include

cyclooxygenase inhibitors such as celecoxib for treatment of gastrointestinal and thoracic malignancies, aspirin for the prevention of colorectal cancer (*PIK3CA* mutant tumors in particular), the antidiabetic agent metformin for multiple solid tumors, and statin therapies in gynecologic and breast cancers (2–5). Additionally, the lymphocytotoxic properties of glucocorticoids have resulted in their widespread use in combination regimens for non-Hodgkin's lymphoma.

Itraconazole is an orally bioavailable and well-tolerated azole antifungal in clinical use for decades for the treatment of invasive fungal infections (6). In a broad drug screen, itraconazole emerged as a potent inhibitor of the hedgehog signaling pathway (7,8) which serves as a critical axis in numerous cancers (9). Unlike vismodegib, a hedgehog inhibitor approved for the treatment of advanced basal cell carcinoma (BCC), itraconazole maintains efficacy against many secondary drug-resistant resistant smoothened (SMO) mutations (8). Separately, itraconazole has demonstrated potent inhibition of endothelial cell proliferation and angiogenesis (10–12) which may account for its apparent activity in non-hedgehog dependent malignancies such as prostate and lung cancers.

Clinical studies of itraconazole as an antineoplastic agent have been performed in prostate cancer, BCC, and non-small cell lung cancer (NSCLC). A study using itraconazole 600 mg/day for castrate resistant prostate cancer resulted in decreased Hh pathway activity that correlated with decreased prostate-specific antigen (PSA) levels (13). In a preliminary phase 2 clinical trial, the addition of itraconazole to pemetrexed chemotherapy for second-line treatment of advanced nonsquamous NSCLC resulted in a doubling of progression-free survival (PFS) and a four-fold increase in overall survival (OS) (14). The survival difference reached statistical significance, even though the trial was closed to enrollment prematurely due to practice changes hindering accrual. In an open-label, proof-of-concept study in advanced BCC, itraconazole 400 mg daily for one month produced substantial decreases in Hh pathway activation, proliferation, and tumor size (15).

Because the biologic effects of itraconazole in human lung cancer cannot be entirely extrapolated from preclinical models or from other human malignancies, we conducted a window-of-opportunity, preoperative study of itraconazole in patients with early-stage non-small cell lung cancer (NSCLC) to determine the mechanism of anti-cancer effects and identify predictors of efficacy.

Methods:

Patient selection and study procedures

This study was approved by the University of Texas Southwestern Medical Center Institutional Review Board (STU122014–038) and was registered on clinicaltrials.gov (NCT02357836). Following Department of Defense (DOD) guidance, a data and safety monitoring committee comprising individuals not directly involved with the study was established. The full protocol was reviewed and approved by the U.S. Army Medical Research and Material Command, Office of Research Protections. All patients provided written informed consent and were recruited and enrolled in the Harold C. Simmons

Comprehensive Cancer Center at UT Southwestern Medical Center in Dallas, Texas. This study was conducted in accordance with ‘Declaration of Helsinki’.

Up to 15 eligible patients were planned for enrollment, with a target of 10 cases with completion of treatment and all biomarker studies. Key eligibility criteria included NSCLC planned for surgical resection, performance status ECOG 0–2, adequate hepatic and renal function, ability to undergo magnetic resonance imaging (MRI) studies, and no concurrent use of medications significantly affecting the metabolism of itraconazole. Although some antiangiogenic agents (eg, bevacizumab) have demonstrated safety concerns (hemoptysis) in squamous histology (16) we enrolled all histologic subtypes because itraconazole had an established safety profile for the treatment of lung abscesses in the setting of lung squamous cell cancer (17,18).

Supplemental Figure 1 shows the study schema. Briefly, prior to initiation of itraconazole, patients underwent dynamic contrast enhanced (DCE)) magnetic resonance imaging (MRI), 4-mm skin punch biopsy, and collection of peripheral blood. Archival tissue from the diagnostic biopsy was obtained. Subjects then received itraconazole 600 mg orally daily (administered as 300 mg orally twice daily) with food for 7–10 days. This dose, higher than the anti-angiogenic dose of itraconazole (14) has been shown to inhibit the Hh pathway in human studies (13). The duration of itraconazole therapy was selected to provide sufficient drug exposure to reach near steady-state pharmacokinetics (PK) in plasma and tissues without significantly delaying surgery. It was also expected to be sufficient for target pharmacodynamic effects, as tumor *Gli1* mRNA has been shown to decrease after as little as 3 days of itraconazole treatment in medulloblastoma xenografts (7). Blood samples were collected for PK analysis. After 7–10 days of itraconazole therapy, subjects underwent repeat DCE MRI, skin punch biopsy, and blood collection. They then resumed itraconazole for 2–3 days, followed by surgical resection. Any standard post-operative therapy and clinical surveillance was determined by patients’ treatment teams.

Specimen handling

Plasma samples with EDTA were centrifuged at 1,100 × g (relative centrifugal force) for 15 min at 4°C for separation of plasma and mononuclear cell layers. Plasma was stored at −70°C. Before analysis, samples were thawed overnight at 4°C and centrifuged at 1,500 × g to remove debris. Skin punch biopsy specimens were flash frozen for RNA procurement (PCR). Research specimens from surgically resected tumors were divided, with half flash-frozen in liquid nitrogen (for PK analysis) and half fixed in 4% paraformaldehyde (for angiogenic marker IHC). Individuals performing and overseeing correlative studies were blinded to patient identity and clinical effects of itraconazole.

Imaging studies

DCE-MRI is an established technology to assess microvessel density (MVD) and tumor capillary permeability (19). Each consented participant was screened for renal disease either by completing a Choyke Questionaire (20) or undergoing point-of-care creatinine testing on the day of the examination. Scans were performed on a 3.0 Tesla Phillips whole-body scanner using a three-dimensional (3D) spoiled gradient echo sequence combined with

parallel imaging, i.e., SENSE technique. Anatomic imaging of the lungs was obtained with breath-held axial and coronal T2-weighted half-Fourier single-shot turbo spin-echo images (SSTSE) acquired with in-plane resolution of 1.5 × 2 mm^2, and slice thickness of 5 mm. These images were used to determine tumor length (i.e., maximum dimension). Because calculated tumor volume can be unreliable due to irregular tumor shape, we calculated the whole tumor volume after segmenting the tumor on each slice where the tumor was visible using the volume tool on the open-source dicom viewer Horos v2.1.1 (21,22). Diffusion weighted imaging (DWI) and arterial spin labelled (ASL) acquisitions were obtained but provided no valuable information (data not shown). Then, the DCE-MRI imaging acquisition plane was set in the oblique sagittal plane so that the target tumor moved along the imaging plane with patient's respiration. Images were acquired before, during and after intravenous administration of a standard dose of 0.1 mmol/kg of gadobutrol (Bayer Heathcare, Wayne, NJ) with subjects in the supine position. Patients were instructed to perform intermittent breath-holds with free-breathing in between. Imaging parameters were as follows: repetition time/echo time: 2.4/1.1 ms; flip angle: 10 degrees; receiver bandwidth: 1857 Hz/pixel; field of view: 320 × 260 mm^2; acquisition voxel size: 2×2 ×4 mm^3; dynamic temporal resolution: 2.6 sec. A total of 90 dynamic frames were acquired. To estimate tumor vascular measures, the extended Tofts model was used on a center slice for each tumor to compute the volume transfer constant (K^{trans}), which reflects the efflux rate of gadolinium contrast from blood plasma into the tissue extravascular extracellular space, using PMI [Sourbron S, Biffar A, Ingrisch M, Fierens Y, Luypaert R. PMI: platform for research in medical imaging. Magn Reson Mater Phys Biol Med 2009;22(suppl 1):539].

Pharmacokinetics

On Day 5, 6, 7, or 8, plasma samples were obtained at approximately 0, 2, 3 and 4 hours following a 300 mg oral dose of itraconazole. We determined plasma and tissue levels of itraconazole and its primary metabolite, hydroxyitraconazole, using a validated ultra-performance liquid chromatography-mass spectroscopy-mass spectroscopy (UPLC-MS/MS) method (23). We considered the duration of itraconazole therapy to be sufficient to achieve steady state, based on a half-life of 24–30 hours (24). PK estimates (area under the time-concentration curve calculated from 0 to 4 hours [$AUC_{0–4h}$], maximum concentration [C_{max}]) and PK parameters (such as clearance, volume, and half-life [$t_{1/2}$]) for itraconazole were calculated using the PK modeling program WinNonlin® 6.1 (Pharsight Corporation, Mountain View, CA). Data were expressed as the means of the relevant measure and/or parameter and inter-individual variances. Additional detail regarding PK methodology is provided in Supplemental Methods.

Cytokine-chemokine analysis

As performed in earlier studies (25), we employed a commercially available kit to measure plasma cytokine and angiogenic factor levels. Kits (human group I, 27-plex cytokine panel [Bio-Rad]) and human group II, 23-plex cytokine panel [Bio-Rad]) were used according to manufacturer instructions using a BioPlex 200 machine (Bio-Rad). Percent change of cytokine levels of post-itraconzole compared to pre-itraconazole treated samples were plotted as a heat map in GraphPad Prism.

Immunohistochemistry

Tissues were fixed in 4% formalin, washed in phosphate-buffered saline (PBS), and embedded in paraffin. 5-μm sections were cut and stained with routine hematoxylin and eosin (H&E). Tissues were deparaffinized and re-hydrated. After antigen retrieval (using DAKO target retrieval solution: cat# S1699) and blocking of endogenous peroxidase activity, biotin, and non-specific proteins with 20% Aquablock (East Coast Biologicals), tissues were incubated in primary antibody (5–10 μg/ml) overnight at 4°C.

Briefly, sections were first deparaffinized and subjected to antigen retrieval as detailed by Sorrelle et al. (26). The sections were incubated with rabbit anti-human CD31 (abcam ab81289, dilution 1:40,000), washed and developed TSA detection system using OPAL 570. The sections were then incubated with mouse anti-human CD31 (Abcam ab9498, dilution 1:250) and subsequently developed with OPAL 520. The sections were counter stained with DAPI and imaged. Images of DAPI, CD31 and CD34 were taken of the same field of view and then merged. Co-localization of CD31 and CD34 were determined using Fiji software as reported by Sorrelle et al. (26).

Metabolic analysis

Three fragments per tissue were mechanically homogenized in 80% MeOH. Fragments were centrifuged at 14,000*g* for 15 min (4 °C). The supernatant was transferred to a new tube and evaporated to dryness using a SpeedVac concentrator (Thermo Savant). Metabolites were reconstituted in 100 μl of 0.03% formic acid in LCMS-grade water, vortex-mixed and centrifuged to remove debris. LC–MS/MS and data acquisition were performed using an AB QTRAP 5500 liquid chromatography/triple quadrupole mass spectrometer (Applied Biosystems SCIEX) with an injection volume of 20 μl, as described previously (27). Chromatogram review and peak area integration were performed using MultiQuant software version 2.1 (Applied Biosystems SCIEX). The peak area for each detected metabolite was normalized against the total ion count of that sample to correct for any variations introduced by sample handling through instrument analysis. The normalized areas were used as variables for the multivariate and univariate statistical data analysis. All multivariate analyses and modelling on the normalized data were carried out using Metaboanalyst 4.0 (http://www.metaboanalyst.ca).

Hedgehog pathway characterization

We analyzed frozen treated tumor tissue and serial skin biopsies for *GLI1* and *PTCH1* mRNA by qPCR. Originally, we had planned to analyze serial tumor specimens as well, but the requirement for a fresh, study-specific baseline biopsy before itraconazole initiation proved impractical. Total RNA was extracted using TriZol (Invitrogen) and purified with PureLink RNA Mini Kit (Invitrogen). cDNA was generated using Superscript III First Strand Synthesis System (Invitrogen). qPCR was performed using Bio-Rad CFX real-time cycler and SYBR Green Master Mix (Bio-Rad). Data are presented as fold change relative to control samples using the ΔΔCt ($2^{-\Delta\Delta Ct}$) method with *HPRT1* as an internal control gene. Primer pairs for qPCR are: (1) *GLI1:* 5’- AGCCGTGCTAAAGCTCCAGT, 5’- CCCACTTTGAGAGGCCCATAG; (2) *PTCH1:* 5’- GGACACTCTCATCTTTTGCTG, 5’- GGTAGTCTGCTTTCTGGGT; and (3) *HPRT1:* 5’- GGTCAGGCAGTATAATCCAAAG,

5’- GGACTCCAGATGTTTCCAAAC. For skin biopsy specimens, we compared pre- and post-treatment specimens. For tumor specimens, we compared resected itraconazole treated lung tumor specimens to untreated NSCLC tumor specimens and normal lung samples that were obtained from the Harold C. Simmons Comprehensive Cancer Center Tissue Resource.

Statistical analyses

To determine effects of itraconazole on tumor angiogenesis, we used paired *t*-tests or Wilcoxon signed rank-tests to investigate if there is a significant change in the values of tissue and peripheral blood samples, and imaging from pre-treatment to post-treatment. To determine effects of itraconazole on the Hedgehog pathway, we used paired *t*-tests to pre- and post-treatment skin biopsies for *GLI1* and *PTCH1* mRNA levels. Spearman’s rank correlation was computed to investigate the association between PK parameters and changes in tumor volume, cytokine, GM-CSF, and tumor microvessel density. We employed the nonlinear mixed effects model to determine the effect of itraconazole pharmacokinetics (PK) on the pharmacodynamic profile of itraconazole. As with similar biomarker studies (25,28), due to the exploratory nature of this study we did not adjust for multiple comparisons.

We planned to enroll up to 15 patients. A sample size of 10 patients provides 90% power to detect a 30% reduction in MVD between the pre-and post-itraconazole tissue samples, assuming a standard deviation of 25% using a paired t-test with a two-sided significance level of 0.05. We considered this a relatively conservative estimate of effect size, as itraconazole reduces MVD by 50–75% in preclinical lung cancer models.(10) Up to five additional patients were planned for accrual as needed to ensure 10 matched pairs of imaging, blood, and tissue data for analysis. The planned total sample size of 15 patients was also consistent with U.S Food and Drug Administration (FDA) recommendations for human PK studies. Specifically, the number of subjects was projected to provide (1) 20% precision (SEM) within PK parameters, and (2) a reasonable understanding of intra-individual variability in pharmacokinetic parameters (29).

Results

Thirteen patients were enrolled to the study. Median age was 64 years, and 9 were female. Additional baseline case characteristics are shown in Table 1. All patients initiated itraconazole therapy. Median total duration of therapy was 12 days (range 8–14 days). With one exception, all patients were entirely adherent to the dosing regimen of 300 mg orally twice daily. The remaining patient, misunderstanding therapy instructions, took only half of the intended dose (300 mg orally once daily). Itraconazole was well tolerated. Reported toxicities included fatigue, nausea, and elevated transaminase levels, all of which were low-grade, reversible, and manageable with standard supportive measures. No complications were reported from study-related skin biopsies, DCE-MRI scans, or blood draws. There were no bleeding or thrombotic complications related to surgery.

PK Analysis

The method validation parameters for determination of itraconazole and hydroxyitraconazole in plasma and tissue met all acceptance criteria for sensitivity,

selectivity, matrix effect, linearity, accuracy, precision, recovery, dilution integrity and stability as set forth in the FDA's May 2018 Guidance for Industry on "Bioanalytical Method Validation" (https://tinyurl.com/rvd9m9f). A representative set of chromatograms are presented in Supplemental Figure 2.

Plasma samples were available for 11 patients and tissue samples were available for 9 patients. The determined PK parameters for itraconazole are presented in Supplemental Table 1a and for hydroxyitraconazole in Supplemental Table 1b. In general, the plasma concentrations of hydroxyitraconazole were higher than that of itraconazole, consistent with previous studies of orally administered itraconazole (30). The steady state concentrations demonstrated relatively low intra-patient variability. However, we did observe relatively high inter-patient variability, with PK parameters varying more than six-fold across patients. It is noteworthy a single subject (Patient #5) self-administered 300 mg/day versus the intended 600 mg/day; therefore, this patient's exposure was significantly less than that of other patients. Other clinical parameters, including body mass index, body surface area, renal function, and hepatic function, did not account for the inter-patient variability in itraconazole concentrations. Concentrations of itraconazole and hydroxyitraconazole for individual patients are shown in Supplemental Figure 2. Table 2 displays significant associations between plasma and tissue concentrations of itraconazole, hydroxyitraconazole, and correlative studies. In general, tissue concentrations of itraconazole and hydroxyitraconazole trended with the plasma concentrations.

Imaging Analysis

Nine patients completed pre- and post-itraconazole MRI studies. Reasons that enrolled patients did not complete paired research MRI scans included presence of metal implants, inadequate renal function, and patient preference. Supplemental Table 2 shows MRI measurements, including tumor length, volume, and K^{trans}. Representative examples of imaging studies are displayed in Figure 1. We observed a wide range of changes in tumor volume (−26% to +13%) and perfusion (−29% to +59%) across cases. With the exception of one case, tumor volume and perfusion changed in the same direction (overall Spearman correlation 0.77; P=0.03). There was a significant association between itraconazole maximal plasma concentration (C_{max}), area under the curve calculated from 0 to 4 hours ($AUC_{0–4h}$), tissue concentration and hydroxy-itraconazole average plasma concentration (C_{ave}) and tumor volume reduction (Spearman rank correlation −0.71; P=0.05) (Table 2). Tissue concentration of itraconazole also significantly associated with change in tumor perfusion (ΔK^{trans}) (correlation −0.71; P=0.01) (Table 2).

Tumor microvessel density

We used CD31 and CD34 co-localization (Supplemental Figure 3) to quantify tumor MVD because CD31 staining alone identified both endothelial cells and non-endothelial cells (data not shown). Figure 2A shows pre- and post-itraconazole MVD by individual patient. Samples for paired pre-and post-itraconazole tumor microvessel density (MVD) were available for 10 patients. As with tumor volume and perfusion, we observed a wide range of changes in MVD, with three cases demonstrating at least 2-fold increase and six cases demonstrating at least 2-fold decrease after itraconazole treatment. Similar to the imaging

parameters, MVD changes were strongly and significantly correlated with PK parameters (Table 2). Specifically, the greater the plasma or tissue itraconazole levels, the greater the decrease in MVD. Changes in MVD were highly correlated with reduction in tumor volume (Spearman correlation 0.77; P=0.03). Additionally, changes in MVD correlated positively with changes in the pro-angiogenic cytokines IL-1β (31) (Spearman correlation 0.57; P=0.05) and GM-CSF(32) (correlation 1.00; P<0.001).

Cytokine-Chemokine Analysis

Cytokine changes over the course of therapy are shown in Figure 2B. Changes in concentrations of the pro-angiogenic cytokines IL-1β (31) (Spearman correlation 0.7; P=0.03), G-CSF(33) (correlation 0.67; P=0.05), and GM-CSF (32) (correlation 1.0; P<0.001) were significantly correlated with tumor volume reduction. Additionally, changes in IL-1β, GM-CSF, and the anti-angiogenic cytokine IFN-γ (34) were significantly associated with PK parameters in such a way that greater itraconazole concentrations were associated with reduced pro-angiogenic and increased anti-angiogenic factors (Table 2).

Hedgehog Pathway Analysis

Twelve patients underwent paired skin biopsies and analyzed for Hh pathway activity. In general, itraconazole therapy did not appear to impact Hh pathway activity as measured by transcription of pathway target genes, *GLI1* and *PTCH1*. In pre- and post-treatment skin biopsies, there was no change in transcription of *GLI1* (P=0.20) and *PTCH1* (P=0.34) mRNA (Figure 3A, B; Supplemental Figure 4). Comparison of itraconazole-treated tumors, normal lung and untreated NSCLC tumors from separate unrelated sample sets demonstrated no significant decrease in *GLI1 and PTCH1* mRNA expression with itraconazole treatment (Figure 3 B, C).

Metabolic Analysis

Resected tumors from six patients (11 tumor regions) underwent metabolic analysis. These were compared to seven resected untreated NSCLC tumors (8 tumor regions). Both principal component analysis (PCA) and partial least squares discriminant analysis (PLS-DA) demonstrated distinct metabolic profiles between treated and untreated tumors (Figure 4A, B). It was interesting that itraconazole impacted some of the same metabolites in both the tumor and the lung, suggesting that the drug has metabolic effects in non-malignant tissue. Several tricarboxylic acid (TCA) cycle metabolites (citrate, succinate, glutamate and malate) were relatively depleted in itraconazole-treated conditions. Furthermore, we observed an accumulation of some metabolites related to ketone metabolism, including L-Acetyl Carnitine and β-hydroxybutyrate.

Discussion

Itraconazole, an antifungal agent in clinical use for more than 25 years, has demonstrated promising anti-tumor efficacy in patients with prostate, lung, and basal cell skin cancer (13–15). Preclinical studies have identified effects on angiogenesis and the Hedgehog pathway as potential mediators of these anti-cancer effects (7,8,10–12). To elucidate the therapeutic mechanism of itraconazole in NSCLC and to identify potential correlates of efficacy, we

performed this pre-operative “window-of-opportunity” trial focused on intensive biospecimen analysis. At higher than standard doses, itraconazole was well tolerated. Although we did not discern any effects on the Hh pathway, we did detect early signals of anti-angiogenic and anti-tumor effects, evidenced by changes in tumor MVD, angiogenic cytokines, perfusion, and volume.

Most notably, we observed a strong and significant association between drug exposure and these potential benefits. Itraconazole concentrations, which varied more than six-fold across cases, were significantly correlated with multiple imaging, tissue, and cytokine parameters, with correlation coefficients ranging 0.6–1.0. The patient with the lowest drug concentrations experienced the greatest increase in tumor volume over the course of the study (Patient #5, Supplemental Tables 1 and 2), whereas the patient with the highest drug concentrations achieved the greatest decrease in tumor volume (Patient #10, Supplemental Tables 1 and 2). The natural history of malignancy and longstanding dose-response principles may account for these observations. In preclinical tumor models, clear proliferation of blood vessels may occur over as little as four days (35). Reviews and meta-analyses of oncology phase 1 clinical trials have shown that the clear majority of responses occur at doses ≥75% of the maximum tolerated dose (36,37). We also observed that intratumoral itraconazole concentrations exceeded those in plasma in all cases. As expected, levels of the active metabolite, hydroxyitraconazole, exceeded that of the parent drug.

The plasma itraconazole levels on day 6 and 11 of our study represent ~80% and 95% of steady state levels (38) and thus, the large variance in plasma and tumor concentrations are unlikely be explained by the inability to reach steady state levels of itraconazole by the end of the patients’ study period. However, despite the low number of patients and large variance of itraconzole levels, our study identified several significant biological correlates with itraconazole levels. Future trials with larger cohorts of patients and longer duration of therapy may identify greater numbers of significant biological correlates and further elucidate itraconazole biology in NSCLC.

Reasons for the wide range in PK parameters are not clear. Apart from a single case in which a patient misunderstood dosing directions and therefore ingested one-half the intended daily dose over the course of the study, dosing diaries and pill counts suggested 100% adherence. Furthermore, patient size, renal function, and hepatic function were not associated with itraconazole concentrations. To our knowledge, patients were not taking concurrent medications known to interact with itraconazole. Nevertheless, unpredictable and heterogeneous itraconazole PK parameters may not be entirely unexpected. In contrast to fluconazole, echinocandins, and polyene antifungals, there is strong evidence supporting the recommendations in favor of monitoring itraconazole levels in both prophylactic and therapeutic contexts. These recommendations for itraconazole reflect clinically meaningful drug exposure-response relationships (39,40) and substantial inherent PK variability, mediated in part by food and gastric pH effects on oral bioavailability of itraconazole (38) as well as potent drug-drug interactions via effects on CYP3A4 (41) PGP1 (41,42) and protein glycosylation (43,44).

The wide range of itraconazole concentrations may also account for the lack of Hh pathway inhibition of skin biopsies and tumors (Fig. 3, Supplemental Fig. 4). Only patients 7 and 10 reached plasma itraconazole levels to those reported on 400 mg daily after 15 days (https://tinyurl.com/ya64msm4) despite taking 600 mg daily. Higher itraconazole levels are required to inhibit the pathway in vivo preclinical studies (7). Furthermore, our study treatment period is also significantly shorter than BCC (15) and prostate cancer (13) trials that treated patients for four to twenty-four weeks and reported Hh pathway inhibition. Biologic effects on target pathways may lag substantially behind PK steady-state as has been shown in studies of EGFR inhibitors (45). Thus, the longer duration of therapy of the latter two studies may have allowed a significant biological effect of the Hh pathway in contrast to our study. Finally, GLI1 activation by other pathways that are independent of the Hh pathway in NSCLC (46,47) may account for lack of tumor activity by itraconazole.

In contrast to bevacizumab and ramucirumab—antibodies approved for NSCLC that target the VEGF ligand and receptor, respectively—itraconazole appears to affect multiple antiangiogenic pathways. Preclinical studies have demonstrated effects on sterol biosynthesis, disruption of cholesterol trafficking, induction of hypoxia inducible factor 1 (HIF1α), and inhibition of VEGF receptor 2 (VEGFR2) and mammalian target of rapamycin (mTOR) pathways (10,11,43). The present clinical trial also suggests broad effects of itraconazole, as we observed exposure-dependent changes in multiple cytokines relevant to vascular biology, including IL-1β, IFNγ, G-CSF, and GM-CSF (31–34) echoing preclinical effects of itraconazole (48,49). Recently, anti-angiogenic agents have received renewed attention in thoracic oncology. In numerous studies, the addition of anti-VEGF or -VEGFR2 therapies to epidermal growth factor receptor (EGFR) inhibitors in *EGFR* mutant NSCLC significantly prolongs disease control (50,51). Furthermore, tumor angiogenesis may have relevance to cancer immunotherapy through effects on T cell infiltration into the tumor microenvironment and immune-regulatory cell function (52).

Our metabolomic assessement of a subset of these patients was hypothesis-neutral because the metabolic effects of itraconazole in lung cancer are unknown. Despite the small cohort, we observed several metabolic differences in itraconazole-treated patients that may indicate a change in the mechanisms of energy formation. The TCA cycle is a central metabolic pathway that allows cells to oxidize metabolic fuels to produce biosynthetic intermediates and energy. Although metabolic activity cannot be inferred directly from metabolite abunance, the relative depletion of several TCA cycle intermediates in itraconazole-treated patients suggests that this pathway functions differently in the presence of the drug. Because NSCLCs use abundant plasma-borne fuels like glucose and lactate to supply the TCA cycle (53,54), the depletion of TCA cycle intermediates could reflect a reduction in the availability of such fuels. The increased abundance of metabolites related to ketone utilization, a pathway that provides alternate fuels when carbohydrate metabolism is impaired, is also consistent with a change in central metabolism in the presence of itraconazole. Interstingly, several of itraconazole's metabolic effects, including its effects on the TCA cycle and ketone-related metabolites, were observed in both the tumor and the adjacent lung, suggesting that they resulted from systemic effects rather than interrutpion in oncogenic signaling in the tumor. Determining whether these metabolic changes are related to

therapeutic responses will require further study in preclinical models and a larger placebo-controlled clinical study.

Pre-operative, phase 0 biomarker studies provide an optimal setting to elucidate pharmacodynamic effects of and predictive biomarkers for emerging cancer therapies. Such studies are particularly essential in lung cancer, where real and perceived challenges to tissue acquisition may hinder implementation of essential biocorrelatives (55). We designed this trial to provide adequate exposure to a novel therapeutic agent, without subjecting patients to a prolonged delay before definitive surgery. The 10–14 days of itraconazole—selected to achieve near steady-state PK—is considerably less than the duration of preoperative gefitinib and pazopanib (up to 42 days) in previously published pre-operative lung cancer studies, both of which were administered to molecularly unselected populations where clinical effects are unknown (25,56). Furthermore, the entire study duration fit well within standard diagnostic and treatment intervals for early-stage lung cancer (57).

Despite these favorable characteristics, we faced challenges performing the intended biomarker studies. For various reasons, including ineligibility for particular studies (eg, renal dysfunction or potential metal implants for research MRI scans) and patient preference, only 9 of the 13 enrolled patients completed all planned biomarker studies. Due to logistical considerations, we eliminated baseline study-specific fresh tumor biopsies. Accordingly, we were not able to perform serial assessment of Hh pathway components in tumor tissue. Whether the Hh analysis in skin biopsies truly represented intratumoral Hh pathway status in this study cannot be determined. However, lack of a fresh pre-treatment biopsy did not affect evaluation of PK or angiogenic parameters. Additionally, in this pre-operative clinical trial, patients did not receive any intervening therapy in between their diagnostic biopsy and the initiation of itraconazole. We would therefore expect the diagnostic biopsy to represent accurately tumor biology at the time study therapy was started. This study design also precluded analysis of tumor metabolomics in paired pre- and post-itraconazole samples. Although we did analyze tumor MVD on archival tumor biopsies, permitting comparison with resected specimens, these small specimens may not be representative of the larger tumor. And while the short duration of study treatment was logistically appealing to patients and providers, it may also pose limitations. Longer therapy may have resulted in greater effects on biomarker endpoints, or may have unearthed other toxicities of high-dose itraconazole. Finally, we recognize the exploratory nature of our findings, which require confirmation in larger clinical trials and biomarker studies.

In conclusion, short-course, high-dose itraconazole exhibited evidence of early anti-vascular and anti-tumor effects that were highly correlated with drug exposure. While reasons for the marked inter-patient variation in itraconazole concentrations observed in this study remain unclear, this observation is consistent with experience in infectious disease settings, where PK variability and clinically meaningful drug exposure-response relationships have led to recommendations for routine monitoring of itraconazole levels. Given the relatively low cost of and accessability to itraconazole (less than $1,000/month, compared to more than $8,000/month for approved anti-angiogenic agents and more than $7,000/month for approved Hh antagonists) (58–60) and growing interest in antiangiogenic therapies across multiple cancer types, further studies incorporating real-time drug monitoring and dose titration are

warranted. More broadly, as the number of fixed-dose cancer therapies increases, attention to inter-patient pharmacokinetic and pharmacodynamic differences may represent important considerations.

Supplementary Material

Refer to Web version on PubMed Central for supplementary material.

Acknowledgements:

The authors thank Ms. Dru Gray for assistance with manuscript preparation and Steven Wright for assistance with IHC.

Funding:

This study was funded by the Department of Defense Lung Cancer Research Program (W81XWH-14-1-0540 to D.E.G.; W81XWH-14-1-0338 to J.K.), National Cancer Institute (NCI) (K24CA201543-01; to D.E.G.; 1R01CA196851 to J.K.), American Cancer Society (RSG-16-090-01-TBG to J.K.), Cancer Prevention Research Institute of Texas Core Facilities Support Award (RP170003; to W.C.P.), Canadian Institutes of Health Research (CIHR) (MFE 140911 to B.F.), NCI (R35CA22044901 to R.J.D), Cancer Prevention Research Institute of Texas (RP160089 to R.J.D.), and the National Heart, Lung, and Blood Institute (5T32HL098040 to S.K.). Additional support provided by the Biomarker Research Core, Tissue Resource, and Biostatistics Shared Resource in the Harold C. Simmons Comprehensive Cancer Center (P30 CA142543; Carlos Arteaga, MD, PI).

References

1. Ponticelli C, Moroni G. Hydroxychloroquine in systemic lupus erythematosus (SLE). Expert opinion on drug safety 2017;16(3):411–9 doi 10.1080/14740338.2017.1269168. [PubMed: 27927040]
2. Mohammed A, Yarla NS, Madka V, Rao CV. Clinically Relevant Anti-Inflammatory Agents for Chemoprevention of Colorectal Cancer: New Perspectives. International journal of molecular sciences 2018;19(8) doi 10.3390/ijms19082332.
3. Liao X, Lochhead P, Nishihara R, Morikawa T, Kuchiba A, Yamauchi M, et al. Aspirin use, tumor PIK3CA mutation, and colorectal-cancer survival. N Engl J Med 2012;367(17):1596–606 doi 10.1056/NEJMoa1207756. [PubMed: 23094721]
4. Chen K, Li Y, Guo Z, Zeng Y, Zhang W, Wang H. Metformin: current clinical applications in nondiabetic patients with cancer. Aging (Albany NY) 2020;12 doi 10.18632/aging.102787.
5. Jeong GH, Lee KH, Kim JY, Eisenhut M, Kronbichler A, van der Vliet HJ, et al. Statin and Cancer Mortality and Survival: An Umbrella Systematic Review and Meta-Analysis. J Clin Med 2020;9(2) doi 10.3390/jcm9020326.
6. Noppen M, Claes I, Maillet B, Meysman M, Monsieur I, Vincken W. Three cases of bronchial stump aspergillosis: unusual clinical presentations and beneficial effect of oral itraconazole. Eur Respir J 1995;8(3):477–80. [PubMed: 7789500]
7. Kim J, Tang JY, Gong R, Kim J, Lee JJ, Clemons KV, et al. Itraconazole, a commonly used antifungal that inhibits Hedgehog pathway activity and cancer growth. Cancer Cell 2010;17(4):388–99 doi 10.1016/j.ccr.2010.02.027. [PubMed: 20385363]
8. Kim J, Aftab BT, Tang JY, Kim D, Lee AH, Rezaee M, et al. Itraconazole and arsenic trioxide inhibit Hedgehog pathway activation and tumor growth associated with acquired resistance to smoothened antagonists. Cancer Cell 2013;23(1):23–34 doi 10.1016/j.ccr.2012.11.017. [PubMed: 23291299]
9. Wu F, Zhang Y, Sun B, McMahon AP, Wang Y. Hedgehog Signaling: From Basic Biology to Cancer Therapy. Cell Chem Biol 2017;24(3):252–80 doi 10.1016/j.chembiol.2017.02.010. [PubMed: 28286127]

10. Aftab BT, Dobromilskaya I, Liu JO, Rudin CM. Itraconazole inhibits angiogenesis and tumor growth in non-small cell lung cancer. Cancer Res 2011;71(21):6764–72 doi 10.1158/0008-5472.CAN-11-0691. [PubMed: 21896639]

11. Xu J, Dang Y, Ren YR, Liu JO. Cholesterol trafficking is required for mTOR activation in endothelial cells. Proc Natl Acad Sci U S A 2010;107(10):4764–9 doi 10.1073/pnas.0910872107. [PubMed: 20176935]

12. Chong CR, Xu J, Lu J, Bhat S, Sullivan DJ Jr., Liu JO. Inhibition of angiogenesis by the antifungal drug itraconazole. ACS chemical biology 2007;2(4):263–70 doi 10.1021/cb600362d. [PubMed: 17432820]

13. Antonarakis ES, Heath EI, Smith DC, Rathkopf D, Blackford AL, Danila DC, et al. Repurposing itraconazole as a treatment for advanced prostate cancer: a noncomparative randomized phase II trial in men with metastatic castration-resistant prostate cancer. Oncologist 2013;18(2):163–73 doi 10.1634/theoncologist.2012-314. [PubMed: 23340005]

14. Rudin CM, Brahmer JR, Juergens RA, Hann CL, Ettinger DS, Sebree R, et al. Phase 2 study of pemetrexed and itraconazole as second-line therapy for metastatic nonsquamous non-small-cell lung cancer. J Thorac Oncol 2013;8(5):619–23 doi 10.1097/JTO.0b013e31828c3950. [PubMed: 23546045]

15. Kim DJ, Kim J, Spaunhurst K, Montoya J, Khodosh R, Chandra K, et al. Open-label, exploratory phase II trial of oral itraconazole for the treatment of basal cell carcinoma. J Clin Oncol 2014;32(8):745–51 doi 10.1200/JCO.2013.49.9525. [PubMed: 24493717]

16. Johnson DH, Fehrenbacher L, Novotny WF, Herbst RS, Nemunaitis JJ, Jablons DM, et al. Randomized phase II trial comparing bevacizumab plus carboplatin and paclitaxel with carboplatin and paclitaxel alone in previously untreated locally advanced or metastatic non-small-cell lung cancer. J Clin Oncol 2004;22(11):2184–91 doi 10.1200/JCO.2004.11.022. [PubMed: 15169807]

17. Smith FB, Beneck D. Localized Aspergillus infestation in primary lung carcinoma. Clinical and pathological contrasts with post-tuberculous intracavitary aspergilloma. Chest 1991;100(2):554–6. [PubMed: 1864137]

18. Malik A, Shahid M, Bhargava R. Prevalence of aspergillosis in bronchogenic carcinoma. Indian journal of pathology & microbiology 2003;46(3):507–10. [PubMed: 15025326]

19. Mamata H, Tokuda J, Gill RR, Padera RF, Lenkinski RE, Sugarbaker DJ, et al. Clinical application of pharmacokinetic analysis as a biomarker of solitary pulmonary nodules: dynamic contrast-enhanced MR imaging. Magn Reson Med 2012;68(5):1614–22 doi 10.1002/mrm.24150. [PubMed: 22231729]

20. Sena BF, Stern JP, Pandharipande PV, Klemm B, Bulman J, Pedrosa I, et al. Screening patients to assess renal function before administering gadolinium chelates: assessment of the Choyke questionnaire. AJR Am J Roentgenol 2010;195(2):424–8 doi 10.2214/AJR.09.3803. [PubMed: 20651199]

21. van der Vorst JR, van Dam RM, van Stiphout RS, van den Broek MA, Hollander IH, Kessels AG, et al. Virtual liver resection and volumetric analysis of the future liver remnant using open source image processing software. World J Surg 2010;34(10):2426–33 doi 10.1007/s00268-010-0663-5. [PubMed: 20652701]

22. Giganti F, Allen C, Piper JW, Mirando D, Stabile A, Punwani S, et al. Sequential prostate MRI reporting in men on active surveillance: initial experience of a dedicated PRECISE software program. Magnetic resonance imaging 2019;57:34–9 doi 10.1016/j.mri.2018.10.013. [PubMed: 30352271]

23. Decosterd LA, Rochat B, Pesse B, Mercier T, Tissot F, Widmer N, et al. Multiplex ultra-performance liquid chromatography-tandem mass spectrometry method for simultaneous quantification in human plasma of fluconazole, itraconazole, hydroxyitraconazole, posaconazole, voriconazole, voriconazole-N-oxide, anidulafungin, and caspofungin. Antimicrobial agents and chemotherapy 2010;54(12):5303–15 doi 10.1128/AAC.00404-10. [PubMed: 20855739]

24. De Beule K, Van Gestel J. Pharmacology of itraconazole. Drugs 2001;61 Suppl 1:27–37. [PubMed: 11219548]

25. Nikolinakos PG, Altorki N, Yankelevitz D, Tran HT, Yan S, Rajagopalan D, et al. Plasma cytokine and angiogenic factor profiling identifies markers associated with tumor shrinkage in early-stage

non-small cell lung cancer patients treated with pazopanib. Cancer Res 2010;70(6):2171–9 doi 10.1158/0008-5472.CAN-09-2533. [PubMed: 20215520]

26. Sorrelle N, Ganguly D, Dominguez ATA, Zhang Y, Huang H, Dahal LN, et al. Improved Multiplex Immunohistochemistry for Immune Microenvironment Evaluation of Mouse Formalin-Fixed, Paraffin-Embedded Tissues. J Immunol 2019;202(1):292–9 doi 10.4049/jimmunol.1800878. [PubMed: 30510069]
27. Mullen AR, Hu Z, Shi X, Jiang L, Boroughs LK, Kovacs Z, et al. Oxidation of alpha-ketoglutarate is required for reductive carboxylation in cancer cells with mitochondrial defects. Cell reports 2014;7(5):1679–90 doi 10.1016/j.celrep.2014.04.037. [PubMed: 24857658]
28. Hanrahan EO, Lin HY, Kim ES, Yan S, Du DZ, McKee KS, et al. Distinct patterns of cytokine and angiogenic factor modulation and markers of benefit for vandetanib and/or chemotherapy in patients with non-small-cell lung cancer. J Clin Oncol 2010;28(2):193–201 doi 10.1200/JCO.2009.22.4279. [PubMed: 19949019]
29. (FDA) USDoHaHSFaDA. 1998 Guidance for Industry--General Considerations for Pediatric Pharmacokinetic Studies for Drugs and Biological Products. <http://www.fda.gov/downloads/Drugs/GuidanceComplianceRegulatoryInformation/Guidances/ucm072114.pdf>.
30. Wiederhold NP, Pennick GJ, Dorsey SA, Furmaga W, Lewis JS 2nd, Patterson TF, et al. A reference laboratory experience of clinically achievable voriconazole, posaconazole, and itraconazole concentrations within the bloodstream and cerebral spinal fluid. Antimicrobial agents and chemotherapy 2014;58(1):424–31 doi 10.1128/AAC.01558-13. [PubMed: 24189246]
31. Voronov E, Shouval DS, Krelin Y, Cagnano E, Benharroch D, Iwakura Y, et al. IL-1 is required for tumor invasiveness and angiogenesis. Proc Natl Acad Sci U S A 2003;100(5):2645–50 doi 10.1073/pnas.0437939100. [PubMed: 12598651]
32. Zheng Q, Li X, Cheng X, Cui T, Zhuo Y, Ma W, et al. Granulocyte-macrophage colony-stimulating factor increases tumor growth and angiogenesis directly by promoting endothelial cell function and indirectly by enhancing the mobilization and recruitment of proangiogenic granulocytes. Tumour biology : the journal of the International Society for Oncodevelopmental Biology and Medicine 2017;39(2):1010428317692232 doi 10.1177/1010428317692232. [PubMed: 28240048]
33. Salcedo R, Young HA, Ponce ML, Ward JM, Kleinman HK, Murphy WJ, et al. Eotaxin (CCL11) induces in vivo angiogenic responses by human CCR3+ endothelial cells. J Immunol 2001;166(12):7571–8 doi 10.4049/jimmunol.166.12.7571. [PubMed: 11390513]
34. Beatty GL, Paterson Y. Regulation of tumor growth by IFN-gamma in cancer immunotherapy. Immunol Res 2001;24(2):201–10 doi 10.1385/IR:24:2:201. [PubMed: 11594457]
35. Siphanto RI, Thumma KK, Kolkman RG, van Leeuwen TG, de Mul FF, van Neck JW, et al. Serial noninvasive photoacoustic imaging of neovascularization in tumor angiogenesis. Opt Express 2005;13(1):89–95 doi 10.1364/opex.13.000089. [PubMed: 19488331]
36. Von Hoff DD, Turner J. Response rates, duration of response, and dose response effects in phase I studies of antineoplastics. Invest New Drugs 1991;9(1):115–22 doi 10.1007/BF00194562. [PubMed: 1827432]
37. Itoh K, Sasaki Y, Miyata Y, Fujii H, Ohtsu T, Wakita H, et al. Therapeutic response and potential pitfalls in phase I clinical trials of anticancer agents conducted in Japan. Cancer Chemother Pharmacol 1994;34(6):451–4 doi 10.1007/BF00685653. [PubMed: 7923553]
38. Barone JA, Koh JG, Bierman RH, Colaizzi JL, Swanson KA, Gaffar MC, et al. Food interaction and steady-state pharmacokinetics of itraconazole capsules in healthy male volunteers. Antimicrob Agents Chemother 1993;37(4):778–84. [PubMed: 8388198]
39. Glasmacher A, Prentice A, Gorschluter M, Engelhart S, Hahn C, Djulbegovic B, et al. Itraconazole prevents invasive fungal infections in neutropenic patients treated for hematologic malignancies: evidence from a meta-analysis of 3,597 patients. J Clin Oncol 2003;21(24):4615–26 doi 10.1200/JCO.2003.04.052JCO.2003.04.052{pii}. [PubMed: 14673051]
40. Denning DW. Treatment of invasive aspergillosis. The Journal of infection 1994;28 Suppl 1:25–33 doi 10.1016/s0163-4453(94)95941-2.
41. Sakaeda T, Iwaki K, Kakumoto M, Nishikawa M, Niwa T, Jin JS, et al. Effect of micafungin on cytochrome P450 3A4 and multidrug resistance protein 1 activities, and its comparison with azole

antifungal drugs. The Journal of pharmacy and pharmacology 2005;57(6):759–64 doi 10.1211/0022357056118. [PubMed: 15969931]

42. Wang EJ, Lew K, Casciano CN, Clement RP, Johnson WW. Interaction of common azole antifungals with P glycoprotein. Antimicrob Agents Chemother 2002;46(1):160–5. [PubMed: 11751127]
43. Nacev BA, Grassi P, Dell A, Haslam SM, Liu JO. The antifungal drug itraconazole inhibits vascular endothelial growth factor receptor 2 (VEGFR2) glycosylation, trafficking, and signaling in endothelial cells. J Biol Chem 2011;286(51):44045–56 doi 10.1074/jbc.M111.278754. [PubMed: 22025615]
44. Frey T, De Maio A. The antifungal agent itraconazole induces the accumulation of high mannose glycoproteins in macrophages. J Biol Chem 2009;284(25):16882–90 doi 10.1074/jbc.M109.007609. [PubMed: 19414590]
45. Wang S, Guo P, Wang X, Zhou Q, Gallo JM. Preclinical pharmacokinetic/pharmacodynamic models of gefitinib and the design of equivalent dosing regimens in EGFR wild-type and mutant tumor models. Mol Cancer Ther 2008;7(2):407–17 doi 10.1158/1535-7163.MCT-07-2070. [PubMed: 18281523]
46. Po A, Silvano M, Miele E, Capalbo C, Eramo A, Salvati V, et al. Noncanonical GLI1 signaling promotes stemness features and in vivo growth in lung adenocarcinoma. Oncogene 2017;36(32):4641–52 doi 10.1038/onc.2017.91. [PubMed: 28368412]
47. Kasiri S, Shao C, Chen B, Wilson AN, Yenerall P, Timmons BC, et al. GLI1 blockade potentiates the antitumor activity of PI3K antagonists in lung squamous cell carcinoma. Cancer Res 2017 doi 10.1158/0008-5472.CAN-16-3315.
48. Muenster S, Bode C, Diedrich B, Jahnert S, Weisheit C, Steinhagen F, et al. Antifungal antibiotics modulate the pro-inflammatory cytokine production and phagocytic activity of human monocytes in an in vitro sepsis model. Life sciences 2015;141:128–36 doi 10.1016/j.lfs.2015.09.004. [PubMed: 26382596]
49. Steinke JW, Liu L, Borish L, Payne S. Itraconazole alters T cell deviation, cytokine production and proliferation. Journal of Allergy and Clinical Immunology 2011;127(2):AB258.
50. Masuda C, Yanagisawa M, Yorozu K, Kurasawa M, Furugaki K, Ishikura N, et al. Bevacizumab counteracts VEGF-dependent resistance to erlotinib in an EGFR-mutated NSCLC xenograft model. Int J Oncol 2017;51(2):425–34 doi 10.3892/ijo.2017.4036. [PubMed: 28627678]
51. Saito H, Fukuhara T, Furuya N, Watanabe K, Sugawara S, Iwasawa S, et al. Erlotinib plus bevacizumab versus erlotinib alone in patients with EGFR-positive advanced non-squamous non-small-cell lung cancer (NEJ026): interim analysis of an open-label, randomised, multicentre, phase 3 trial. Lancet Oncol 2019;20(5):625–35 doi 10.1016/S1470-2045(19)30035-X. [PubMed: 30975627]
52. Manegold C, Dingemans AC, Gray JE, Nakagawa K, Nicolson M, Peters S, et al. The Potential of Combined Immunotherapy and Antiangiogenesis for the Synergistic Treatment of Advanced NSCLC. J Thorac Oncol 2017;12(2):194–207 doi 10.1016/j.jtho.2016.10.003. [PubMed: 27729297]
53. Hensley CT, Faubert B, Yuan Q, Lev-Cohain N, Jin E, Kim J, et al. Metabolic Heterogeneity in Human Lung Tumors. Cell 2016;164(4):681–94 doi 10.1016/j.cell.2015.12.034. [PubMed: 26853473]
54. Faubert B, Li KY, Cai L, Hensley CT, Kim J, Zacharias LG, et al. Lactate Metabolism in Human Lung Tumors. Cell 2017;171(2):358–71 e9 doi 10.1016/j.cell.2017.09.019. [PubMed: 28985563]
55. Campo M, Gerber D, Gainor JF, Heist RS, Temel JS, Shaw AT, et al. Acquired Resistance to First-Line Afatinib and the Challenges of Prearranged Progression Biopsies. J Thorac Oncol 2016;11(11):2022–6 doi 10.1016/j.jtho.2016.06.032. [PubMed: 27553514]
56. Lara-Guerra H, Waddell TK, Salvarrey MA, Joshua AM, Chung CT, Paul N, et al. Phase II study of preoperative gefitinib in clinical stage I non-small-cell lung cancer. J Clin Oncol 2009;27(36):6229–36 doi 10.1200/JCO.2009.22.3370. [PubMed: 19884551]
57. Yorio JT, Xie Y, Yan J, Gerber DE. Lung cancer diagnostic and treatment intervals in the United States: a health care disparity? J Thorac Oncol 2009;4(11):1322–30 doi 10.1097/JTO.0b013e3181bbb130. [PubMed: 19752757]

58. Barnett JC, Alvarez Secord A, Cohn DE, Leath CA 3rd, Myers ER, Havrilesky LJ. Cost effectiveness of alternative strategies for incorporating bevacizumab into the primary treatment of ovarian cancer. Cancer 2013 doi 10.1002/cncr.28283.

59. Herbrecht R, Rajagopalan S, Danna R, Papadopoulos G. Comparative survival and cost of antifungal therapy: posaconazole versus standard antifungals in the treatment of refractory invasive aspergillosis. Curr Med Res Opin 2010;26(10):2457–64 doi 10.1185/03007995.2010.516110. [PubMed: 20822354]

60. Poggi L, Kolesar JM. Vismodegib for the treatment of basal cell skin cancer. Am J Health Syst Pharm 2013;70(12):1033–8 doi 10.2146/ajhp120311. [PubMed: 23719880]

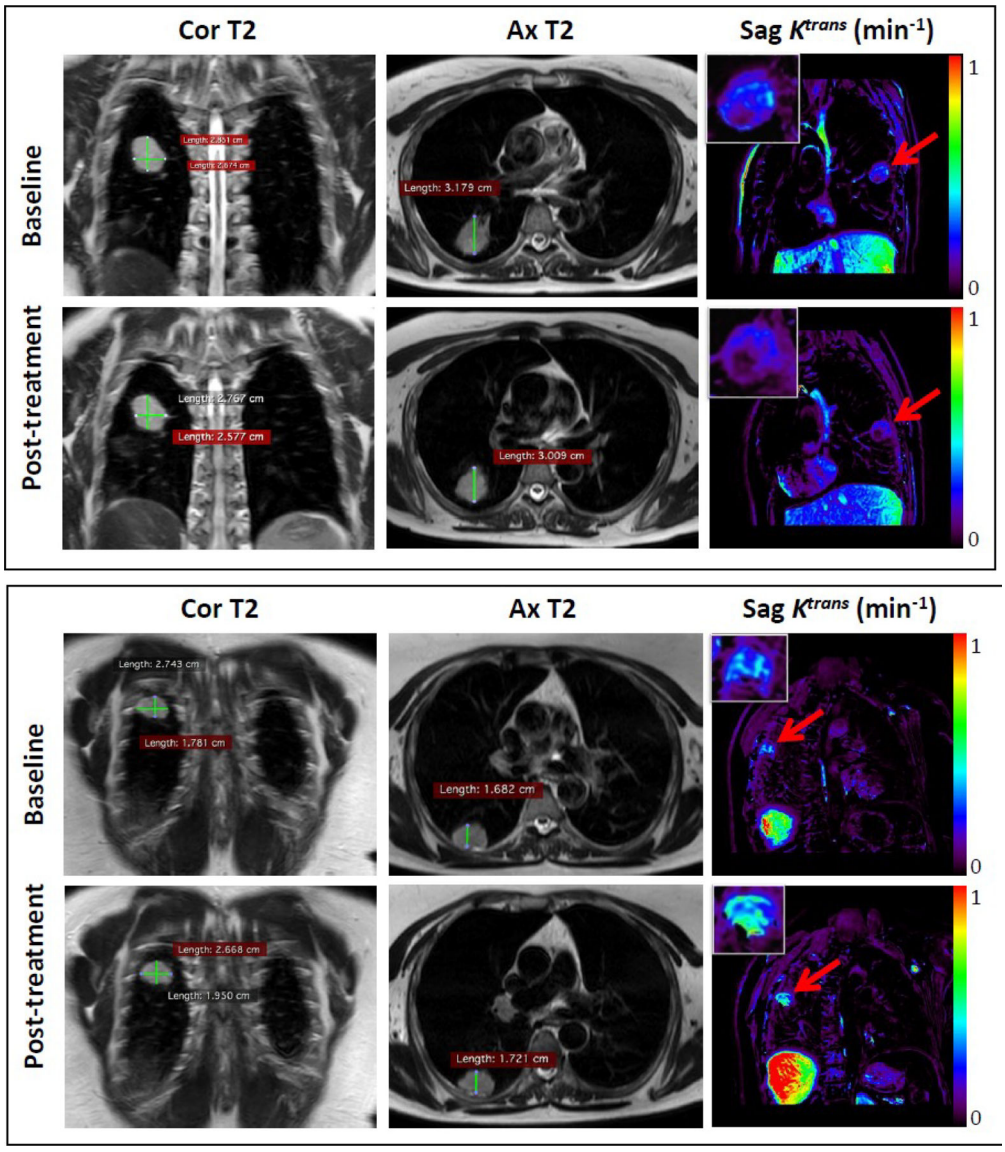

Figure 1. MRI analysis.

Representative coronal (Cor) and axial (Ax) T2-weighted (T2) anatomic images and oblique sagittal (Sag) K^{trans} permeability map generated from DCE-MRI at baseline (upper panels) and after treatment (lower panels) in two different patients. Insets show enlargements of the measured tumors. Patient #3 ***(top)***: Median tumor K^{trans} value at baseline (yellow arrow, upper panel) is 0.17 min^{-1} and post-treatment (yellow arrow, lower panel) is 0.12 min^{-1}. Patient #12 ***(bottom)***: Median tumor K^{trans} value at baseline (yellow arrow, upper panel) is 0.32 min^{-1} and post-treatment (yellow arrow, lower panel) is 0.51 min^{-1}.

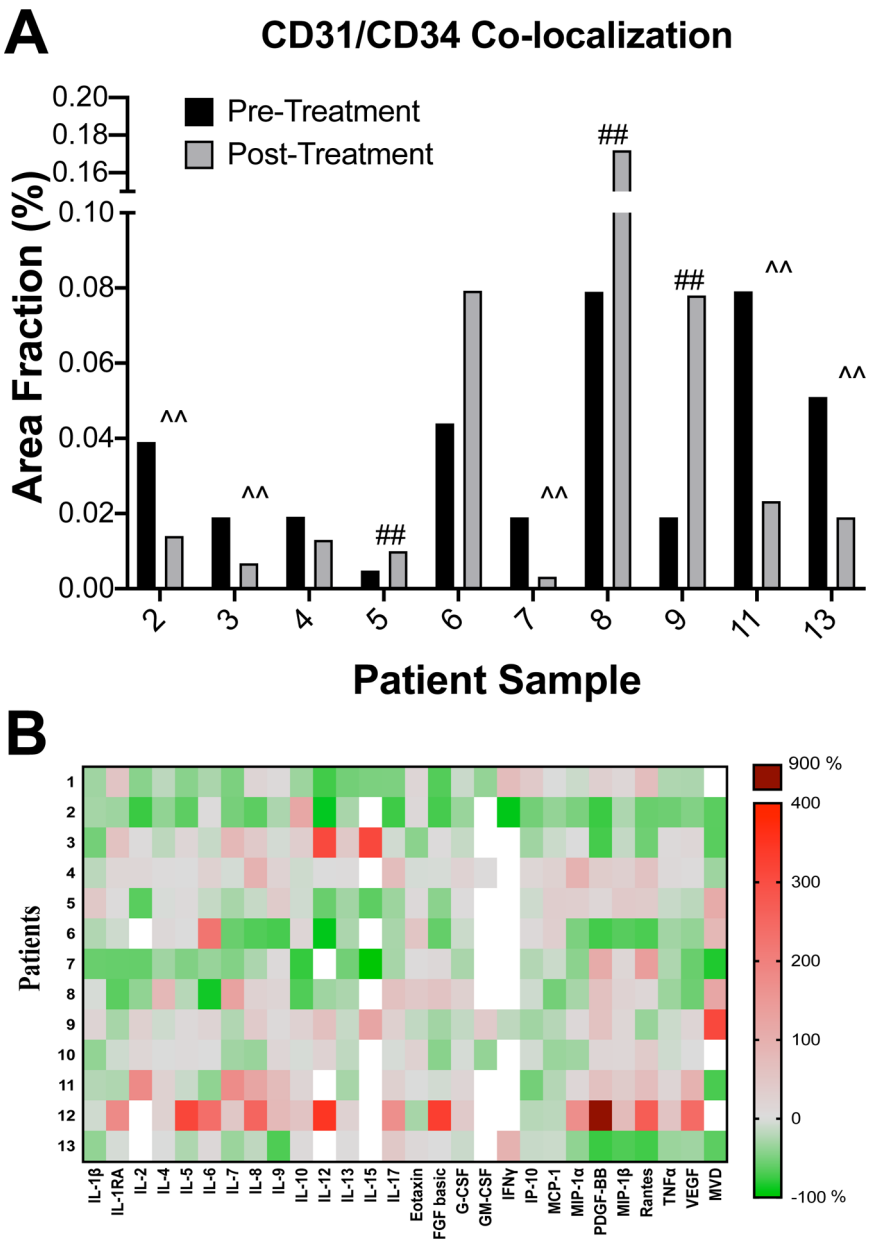

Figure 2. Tumor vascular and plasma cytokine analyses.

(*A*) Tumor microvessel density. Mean of area fraction of CD31 and CD34 co-localized vessels, as a measure of mean vessel density (MVD), for pre- and post-itraconazole treated tumors are shown. CD31 and CD34 were stained by immunohistochemistry of paraffin embedded sections. '##' and '^^' mark cases that demonstrated an increase and decrease, respectively, of at least 2-fold in the mean of area fraction after itraconazole treatment. **(*B*)** Plasma cytokine profiling. Plasma cytokine levels of patients pre- and post-itraconazole were measured with commercially available cytokine panels (see Methods) and compared. Heatmap indicates percent changes in levels of 27 cytokines after itraconazole therapy in 13 patients. Red panels indicate increases in cytokine levels whereas green panels indicate decreases in cytokine levels after itraconazole treatment. White panels indicate cytokine

levels that were undetectable in pre- or post-itraconazole plasma samples. Change in MVD is also indicated.

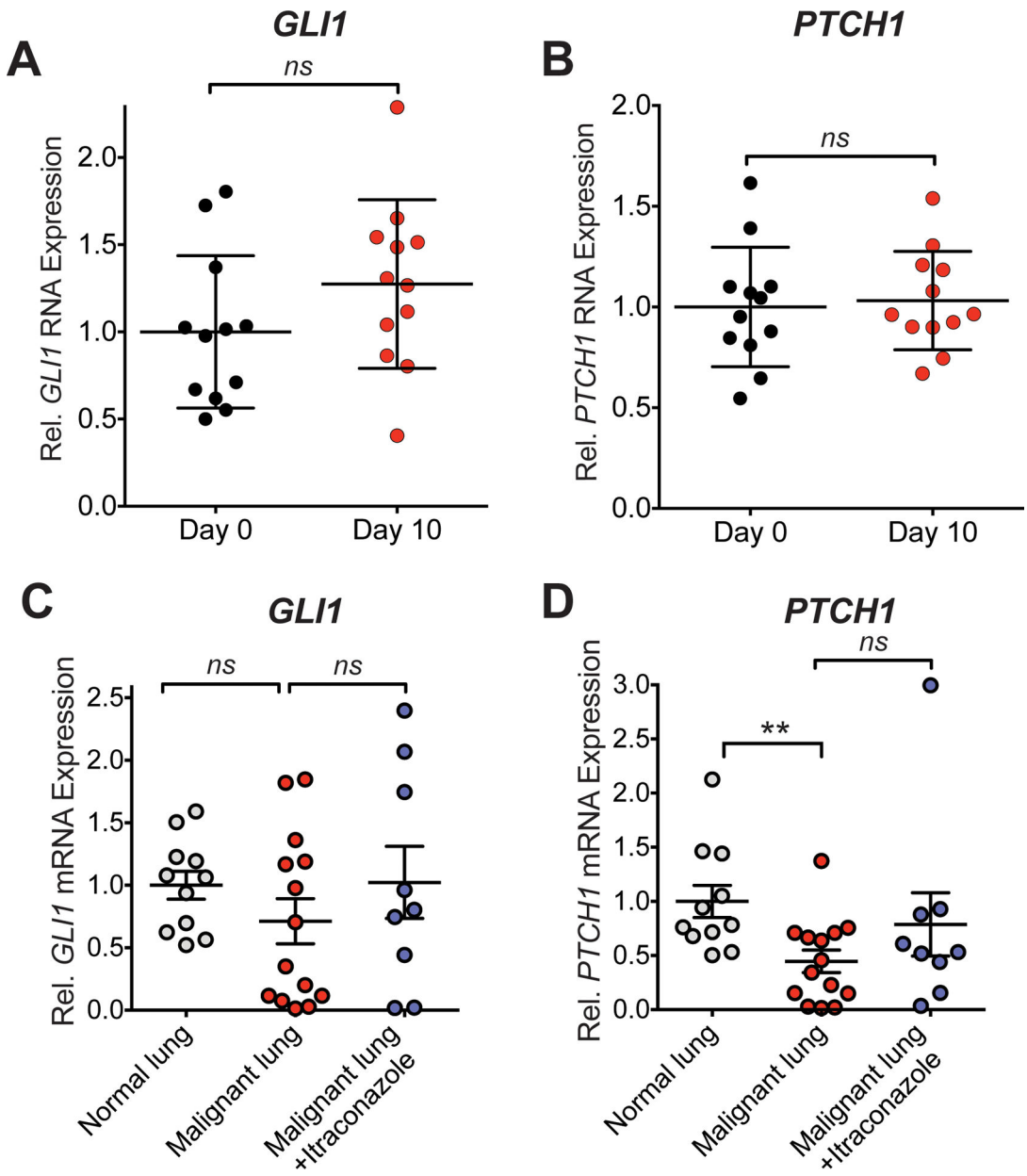

Figure 3. Hedgehog pathway analysis in skin and lung tumor samples.

(A, B) Transcription of *GLI1* (A) and *PTCH1* (B) mRNA, as a readout for Hh pathway activity, in skin biopsies before and after 10 days of itraconazole treatment is shown. All samples were normalized to the mean of respective day 0 mRNA levels. *ns* = not significant. **(C, D)** *GLI1* (C) and *PTCH1* (D) mRNA levels of resected lung tumors treated with itraconazole, lung tumors and normal lung from other unrelated sample sets are shown. ** *P* = 0.004; *ns* = not significant

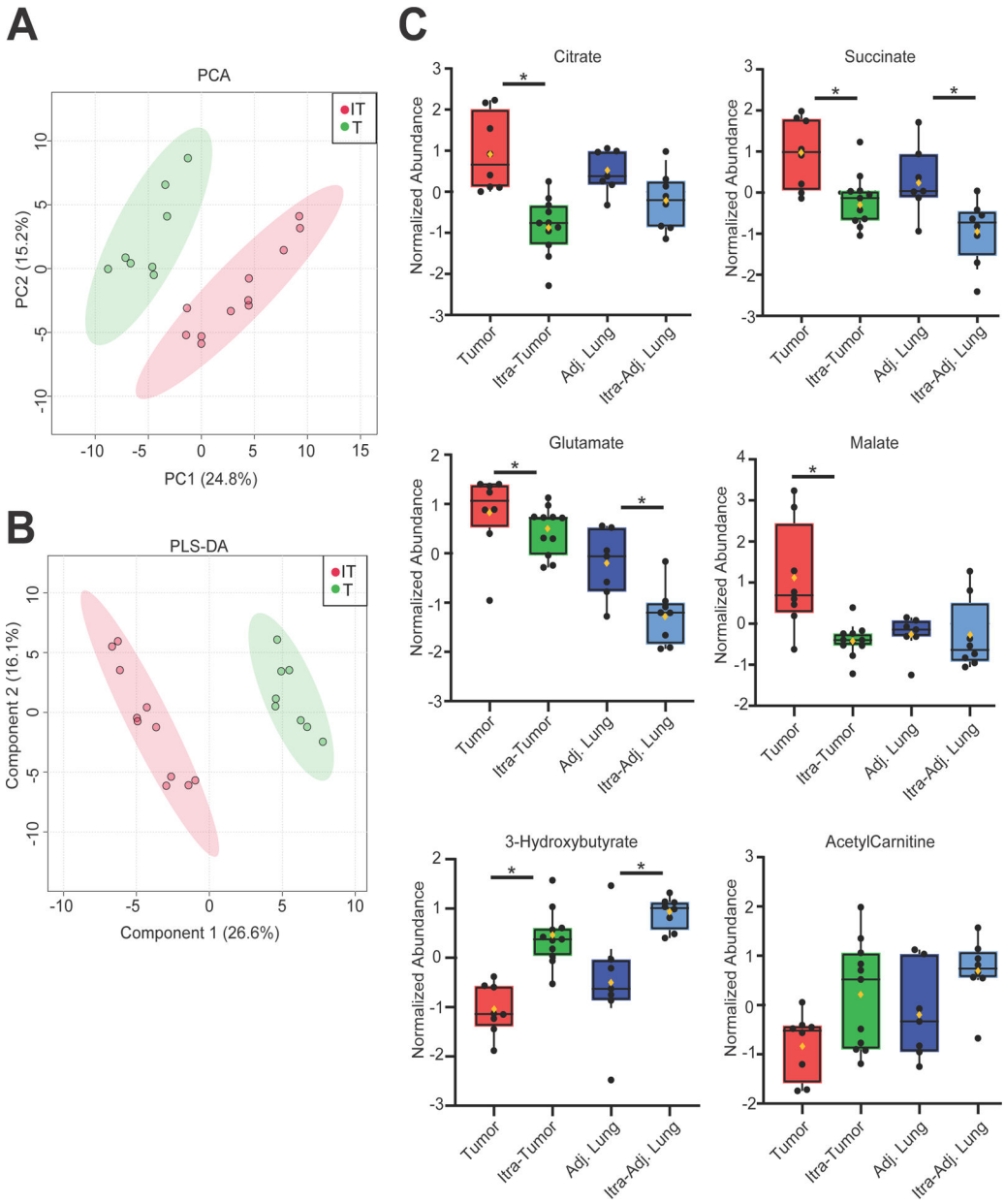

Figure 4. Tumor metabolic analysis.

Treated (*red*) (n=6 patients, 11 tumor regions analyzed) and non-treated (*green*) (n=7, 8 regions) NSCLC. **(A)** Principal Component Analysis (PCA) and **(B)** Partial Least Squares Discriminant Analysis (PLS-DA) are shown. Colored circles represent the average of three independent fragments from an individual tumor region. IT = itraconazole treated tumors. T = untreated tumors. **(C)** Changes in individual metabolites. Black dots indicate the relative abundance of the indicated metabolites. The lines indicate the median and 95% CI. The mean value is indicated by the yellow diamond symbol. Non-treated tumor (red), itraconazole -treated tumor (green), untreated adjacent lung (dark blue) itraconazole-treated adjacent lung (light blue). $*P < 0.05$. Figures were generated using Metaboanalyst 4.0.

Table 1.

Baseline characteristics of 13 patients enrolled in trial.

Characteristic	Number (%) or median (range)
Age (y)	64 (50–80)
Sex	
Female	9 (69)
Male	4 (31)
Race	
White	12 (92)
African-American	1 (8)
Histology	
Adenocarcinoma	9 (69)
Squamous Cell	2 (15)
Other	2 (15)
Smoking History	
Former	10 (77)
Never	3 (23)

Table 2.

Associations between pharmacokinetic (PK) parameters and changes in tumor volume, perfusion (K^{trans}), angiogenic cytokines, and microvessel density.

PK Parameter	Correlative	Correlation*	*P* value
Itraconazole C_{max} (plasma) (ng/mL)	Tumor volume Δ	−0.71	0.05
	Tumor MVD Δ	−0.69	0.03
	GM-CSF Δ	−1.00	<0.001
	IFN-γ Δ	1.00	<0.001
Itraconazole $AUC_{0–4h}$ (plasma) (ng·mL/hr)	Tumor volume Δ	−0.63	0.009
	Tumor MVD Δ	−0.67	0.03
	IL-1β Δ	−0.73	0.01
	IFN-γ Δ	1.00	<0.001
Hydroxyitraconazole C_{ave} (plasma) (ng/mL)	Tumor volume Δ	−0.71	0.05
	IL-1β Δ	−0.78	0.005
	IFN-γ Δ	1.00	<0.001
Itraconazole concentration (tissue) (ng/mL)	Tumor volume Δ	−0.59	0.04
	Tumor K^{trans} Δ	−0.71	0.01
	Tumor MVD Δ	−0.69	0.06

$AUC_{0–4h}$, area under the curve calculated from 0 to 4 hours; GM-CSF, granulocyte macrophage colony stimulating factor; IFN, interferon; MVD, microvessel density

*Spearman rank correlation